AERODYNAMICS AND POLLEN ULTRASTRUCTURE IN *EPHEDRA*[1]

KRISTINA BOLINDER[2,4], KARL J. NIKLAS[3], AND CATARINA RYDIN[2]

[2]Department of Ecology, Environment and Plant Sciences, Stockholm University, Stockholm, SE-106 91, Sweden; and [3]Section of Plant Biology, School of Integrative Plant Science, Cornell University, Ithaca, New York 14853 USA

- *Premise of the study:* Pollen dispersal is affected by the terminal settling velocity (U_t) of the grains, which is determined by their size, bulk density, and by atmospheric conditions. The likelihood that wind-dispersed pollen is captured by ovulate organs is influenced by the aerodynamic environment created around and by ovulate organs. We investigated pollen ultrastructure and U_t of *Ephedra foeminea* (purported to be entomophilous), and simulated the capture efficiency of its ovules. Results were compared with those from previously studied anemophilous *Ephedra* species.
- *Methods:* U_t was determined using stroboscopic photography of pollen in free fall. The acceleration field around an "average" ovule was calculated, and inflight behavior of pollen grains was predicted using computer simulations. Pollen morphology and ultrastructure were investigated using SEM and STEM.
- *Key results:* Pollen wall ultrastructure was correlated with U_t in *Ephedra*. The relative proportion and amount of granules in the infratectum determine pollen bulk densities, and (together with overall size) determine U_t and thus dispersal capability. Computer simulations failed to reveal any functional traits favoring anemophilous pollen capture in *E. foeminea*.
- *Conclusion:* The fast U_t and dense ultrastructure of *E. foeminea* pollen are consistent with functional traits that distinguish entomophilous species from anemophilous species. In anemophilous *Ephedra* species, ovulate organs create an aerodynamic microenvironment that directs airborne pollen to the pollination drops. In *E. foeminea*, no such microenvironment is created. Ephedroid palynomorphs from the Cretaceous share the ultrastructural characteristics of *E. foeminea*, and at least some may, therefore, have been produced by insect-pollinated plants.

Key words: anemophily; entomophily; Gnetales; granular infratectum; pollen morphology; pollination; scanning electron microscopy; scanning transmission electron microscopy; *Welwitschia*.

Pollination involves three distinct processes: pollen release by microsporangiate organs (and sometimes secondary pollen presentation), dispersal of pollen by means of abiotic and/or biotic vector(s), and pollen capture by ovulate organs. In wind pollination, the dispersal distance of a pollen grain is influenced by two factors; the atmosphere surrounding the pollen source, and the terminal settling velocity of pollen (Niklas, 1985). The terminal settling velocity, U_t, of a pollen grain, or any particle, is determined by its size and bulk density (Vogel, 1981). Small pollen grains are generally correlated with slow terminal settling velocities (Hall and Walter, 2011), as is low pollen density, these functional traits increase the time spent by a pollen grain in the air column and thus, all other things being equal, increase dispersal distance (Niklas, 1985; Bolick, 1990; Di-Giovanni et al., 1995; Schwendemann et al., 2007; Cresswell et al., 2010).

The density of the protoplasm of pollen grains is relatively uniform across plant species (Niklas, 1985). Nevertheless, pollen density and U_t vary tremendously, both within and among anemophilous and entomophilous species. Some of this variation is attributable to pollen ultrastructure, which can influence pollen bulk density. In addition, numerous studies have demonstrated a positive correlation between pollination syndrome and exine surface architecture (Hesse, 1981; Ferguson and Skvarla, 1982; Grayum, 1986; Bolick, 1990; Osborn et al., 1991). Airborne pollen generally disperses as small, dry, nonadhesive isolated grains with a smooth rather than sculptured exine (Faegri and van der Pijl, 1979; Whitehead, 1983; Ackerman, 2000; Culley et al., 2002; Friedman and Barrett, 2008). By adding surface area, with only a minor associated addition of mass, the U_t can be reduced (Schwendemann et al., 2007). The two characteristic hollow sacs of *Pinus* L. pollen have been mathematically shown to decrease the settling velocity by increasing the aerodynamic drag forces acting on the grain (Schwendemann et al., 2007). In contrast, insect-borne pollen is generally adhesive

[1]Manuscript received 24 November 2014; revision accepted 5 February 2015.

The authors thank two anonymous reviewers for constructive insights, K. Loefler (Cornell University) for assistance with stroboscopic photography, S. Lindwall (Stockholm University) for laboratory assistance, L. Norbäck-Ivarsson and O. Thureborn (Stockholm University) for providing fresh pollen grains of *Ephedra foeminea*, J. M. Beaulieu (University of Tennessee) for providing the GLS script, A. M. Humphreys (Stockholm University) for fruitful discussions, B. Bremer (Stockholm University) and J. Schönenberger (University of Vienna) for comments on the text, and the curators of the herbaria BM, L, NY, S, W and WU, the Bergius Botanic Garden, and the Botanical Garden of Stockholm University for access to plant material. Funding was provided from the Faculty of Science, Stockholm University, and the Swedish Research Council (to C.R.) and the College of Agriculture and Life Science, Cornell University (to K.J.N.).

[4]Author for correspondence (e-mail: kristina.bolinder@su.se)

doi:10.3732/ajb.1400517

to maximize the number of pollen grains that attach to a vector for transportation (Wodehouse, 1935; Faegri and van der Pijl, 1979; Ackerman, 2000; Culley et al., 2002). This adhesiveness also facilitates the formation of pollen clumps, which consequently increases U_t compared with an individual pollen grain. Indeed, the tendency to form clumps of pollen is considered a good indicator of insect pollination (Hall and Walter, 2011). In light of these generalizations, we examined the ultrastructure and aerodynamics of the pollen of the gymnosperm *Ephedra* L. (Gnetales) and used these functional traits to make inferences about the pollination biology of *E. foeminea* Forssk. (which is purported to be insect-pollinated and reflect the ancestral pollination syndrome in the genus; Bolinder et al., 2014) by comparing these traits with those of species described to be wind-pollinated. Our focus on pollen ultrastructure stems from the intrinsic relationship between pollen form and pollination syndromes.

Ephedra comprises between 50 and 60 species (Kubitzki, 1990). However, despite strong morphological and ecological similarities among species, variation in pollination syndrome has been demonstrated (Bolinder et al., 2014). Although most species are anemophilous (or have been described as such in the literature), the sister species to all other species, *E. foeminea*, is entomophilous (Bolinder et al., 2014). In addition, *E. aphylla* Forssk. is proposed to use a combination of abiotic and biotic pollination (Bino et al., 1984; Meeuse et al., 1990). Pollen of *Ephedra* is characteristically polyplicate and was first described in detail by Wodehouse (1935) and later by Steeves and Barghoorn (1959), Kedves (1987), and Ickert-Bond et al. (2003). Variation in pollen morphology within the genus has long been recognized not only at the species level (Wodehouse, 1935; Steeves and Barghoorn, 1959; Kedves, 1987), but also within individuals and single microsporangia (e.g., El-Ghazaly and Rowley, 1997; Ickert-Bond et al., 2003). The pollen morphology of *Ephedra* is thus considered understudied and poorly defined and understood, particularly in terms of whether different pollen types reflect evolutionary relationships and/or different pollination syndromes. The aperture condition in *Ephedra* is unclear and has been variably described as polyaperturate (Steeves and Barghoorn, 1959; Bharadwaj, 1963) and inaperturate (Erdtman, 1952; Huynh, 1975; Kurmann and Zavada, 1994; El-Ghazaly et al., 1998; Ickert-Bond et al., 2003). When the pollen grain germinates, the exine, including both ectexine and endexine, splits open between the ridges and discards from the intine, which covers the gametophyte (Land, 1907; El-Ghazaly et al., 1998). Between each ridge a furrow is located where the exine is thinner (Figs. 1, 2). This furrow, which can be either branched (Fig. 1B, C, D, F) or unbranched (Fig. 1A, E), will here be called the pseudosulcus, as suggested by Huynh (1975). Preliminary results (Norbäck-Ivarsson, 2014) indicate that pollen morphology is a phylogenetically informative character that can be divided into (at least) two types: the derived pollen type, present for example in the anemophilous species *E. distachya* L., in which the pseudosulci have lateral branches, and the ancestral pollen type, present in a basal grade of taxa including the entomophilous *E. foeminea*, in which the pseudosulci lack side branches.

Our focus on the aerodynamics of *Ephedra* ovules stems from the fact that successful wind pollination is profoundly influenced by the size, orientation, and morphology of ovulate organs just as much as by the physical properties of pollen grains. Although morphological variation within *Ephedra* is generally low, some morphological features of ovulate structures are clade-specific (Rydin et al., 2010). The aerodynamics created around ovulate structures can therefore be unique to clades or species. When the U_t of pollen is quantified and the airflow patterns (i.e., the acceleration field) around an ovulate organ are determined, it is possible to predict the average behavior of pollen inflight trajectories (see, for example, Niklas et al., 1986; Niklas and Kerchner, 1986; Niklas and Buchmann, 1987; Buchmann et al., 1989).

MATERIALS AND METHODS

***Aerodynamic features of* E. foeminea**—*Settling velocity*—Anthetic microsporangiate structures of *E. foeminea* were collected in Croatia on 9 July 2013 and stored in a refrigerator until measurements could be taken. The terminal settling velocity, U_t, was determined by stroboscopic photographing (40 flashes/s), pollen grains falling through a glass cylinder with a diameter of 14 cm (Fig. 3). The height of the column required to achieve U_t was determined based on calculations using average pollen grain dimensions and estimates of cytosol density. These preliminary calculations were necessary to ensure that the photographic images of inflight pollen grains were taken once the grains had reached free fall, i.e., when their body and drag forces were at equilibrium (Niklas and Spatz, 2012). This necessity is seen by considering a pollen grain with density ϱ_s and volume V suspended in air with density ϱ_f. The net body force F_N on this pollen grain equals the difference between its mass and that of the air it displaces times the gravitational constant g. Thus, the net body force equals: $F_N = gV\left(\rho_s - \rho_f\right)$.

In turn, the drag force, D_f, on a very small pollen grain with average diameter d is given by Stokes's formula: $D_f = -3\pi d\upsilon\rho_f U$, where υ is kinematic viscosity and U is the speed at which the grain moves through the air. This last formula holds true for Reynolds numbers ≤1.0. At equilibrium, we see that $F_N + D_f = 0$, which leads to a formula for the terminal velocity:

$$U_t = \frac{gV\left(\rho_S - \rho_f\right)}{3\pi d\upsilon\rho_f}.$$

The U_t of *E. foeminea* pollen grains was calculated by dividing the distance between successive images of free falling grains by the time between successive flashes (online Appendix S1). The U_t of *E. trifurca* Torr. and *E. nevadensis* S.Watson were taken from the literature using the identical protocols as used in this study (e.g., Niklas and Buchmann, 1987). For comparison, U_t was investigated for *Welwitschia mirabilis* Hook. f. (Gnetales), using pollen extracted from microsporangiate structures collected at the Bergius Botanic Garden in Stockholm on 13 November 2013.

Computer simulations of pollen grain motion—The dimensions of 12 ovules from *E. foeminea* (collected in Croatia) were measured (online Appendix S2) and used to simulate the morphology, size, and orientation of an "average" ovule for the purposes of calculating the acceleration field around the ovule. Within 30 h of of collection in Croatia, 134 fully developed and mature pollen grains of *E. foeminea* were mounted on aluminum stubs, sputter coated with gold, and measured using scanning electron microscopy (SEM) (online Appendix S3). The average wind speed during the week *E. foeminea* was at anthesis was 223.5 cm·s^{-1} (measured at Split airport, 25 km from the *E. foeminea* locality); this average wind speed was used as the ambient upwind wind speed in our simulations. Pollen behavior around an ovulate structure was simulated using a program devised by Niklas and Kerchner (for details, see Niklas and Kerchner, 1986). This program predicts the inflight behavior of pollen grains differing in physical properties within the acceleration field created by and around any solid obstruction to airflow. In the case of the simulations reported here, a Cartesian coordinate system consisting of 35 × 27 grid cells was used to define a total of 945 sectors that collectively defines the airspace around an ovule and the volume of space occupied by an ovule. A vertically oriented, "average" ovule, bearing a single pollination droplet, was placed within this airspace. Using an ambient windward speed of 223.5 cm·s^{-1}, airflow speed and direction were then calculated within each grid cell to compute airflow vectors that collectively define acceleration field. The vectors within each three-dimensional grid cell were then used to calculate the most probable trajectories of 500 simulated pollen grains possessing the same size, morphology, and bulk density as

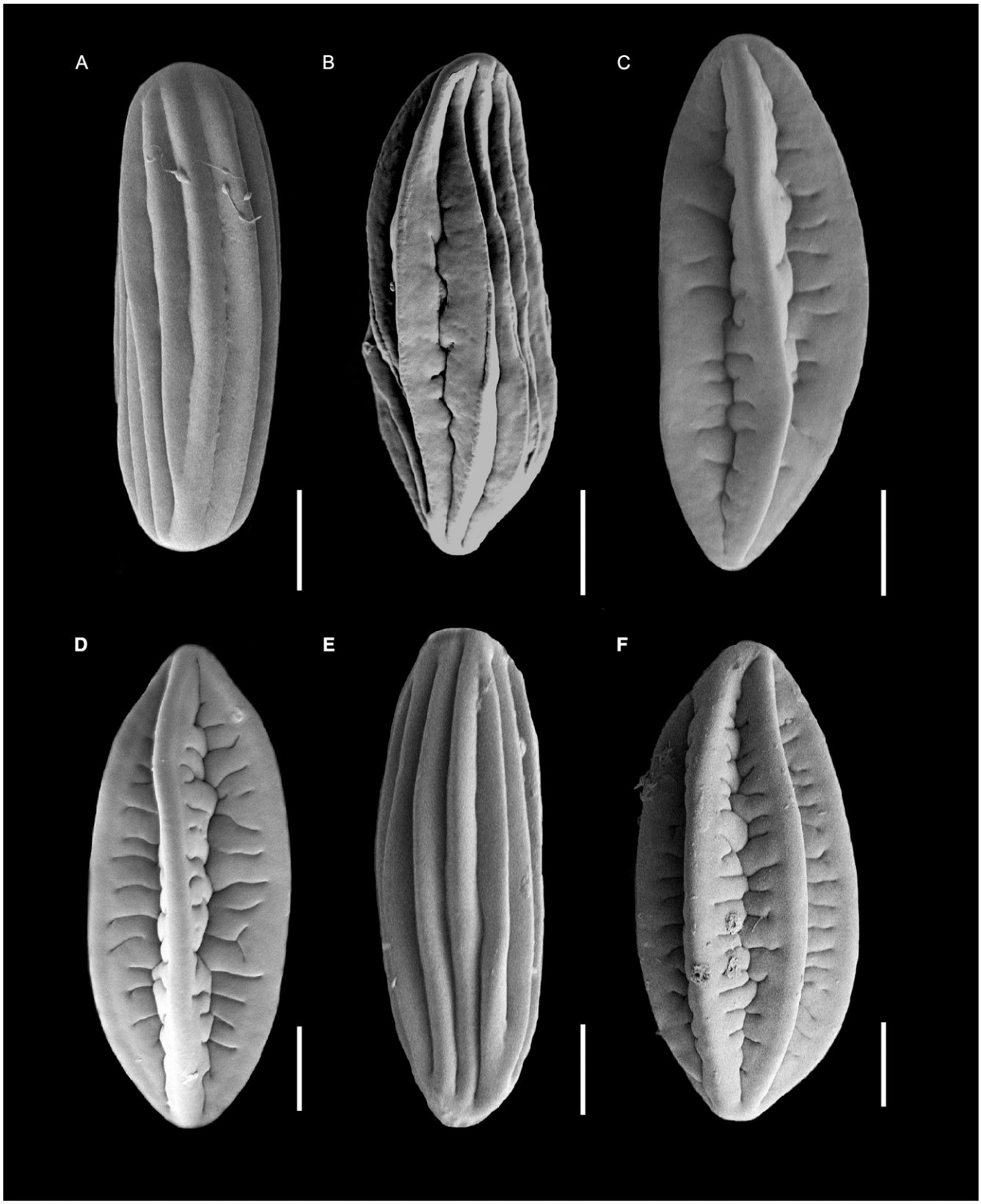

Fig. 1. Scanning electron micrographs of *Ephedra* pollen. (A) *Ephedra foeminea*, (B) *E. likiangensis*, (C) *E. distachya*, (D) *E. viridis*, (E) *E. trifurca*, (F) *E. nevadensis*. *Ephedra foeminea* (A) and *E. trifurca* (E) show the ancestral pollen type with unbranched pseudosulci extending between the plicae along the equatorial axis. *Ephedra likiangensis* (B), *E. distachya* (C), *E. viridis* (D) and *E. nevadensis* (F) show the derived pollen type with branched pseudosulci extending between the plicae along the equatorial axis. Scale bars = 10 μm.

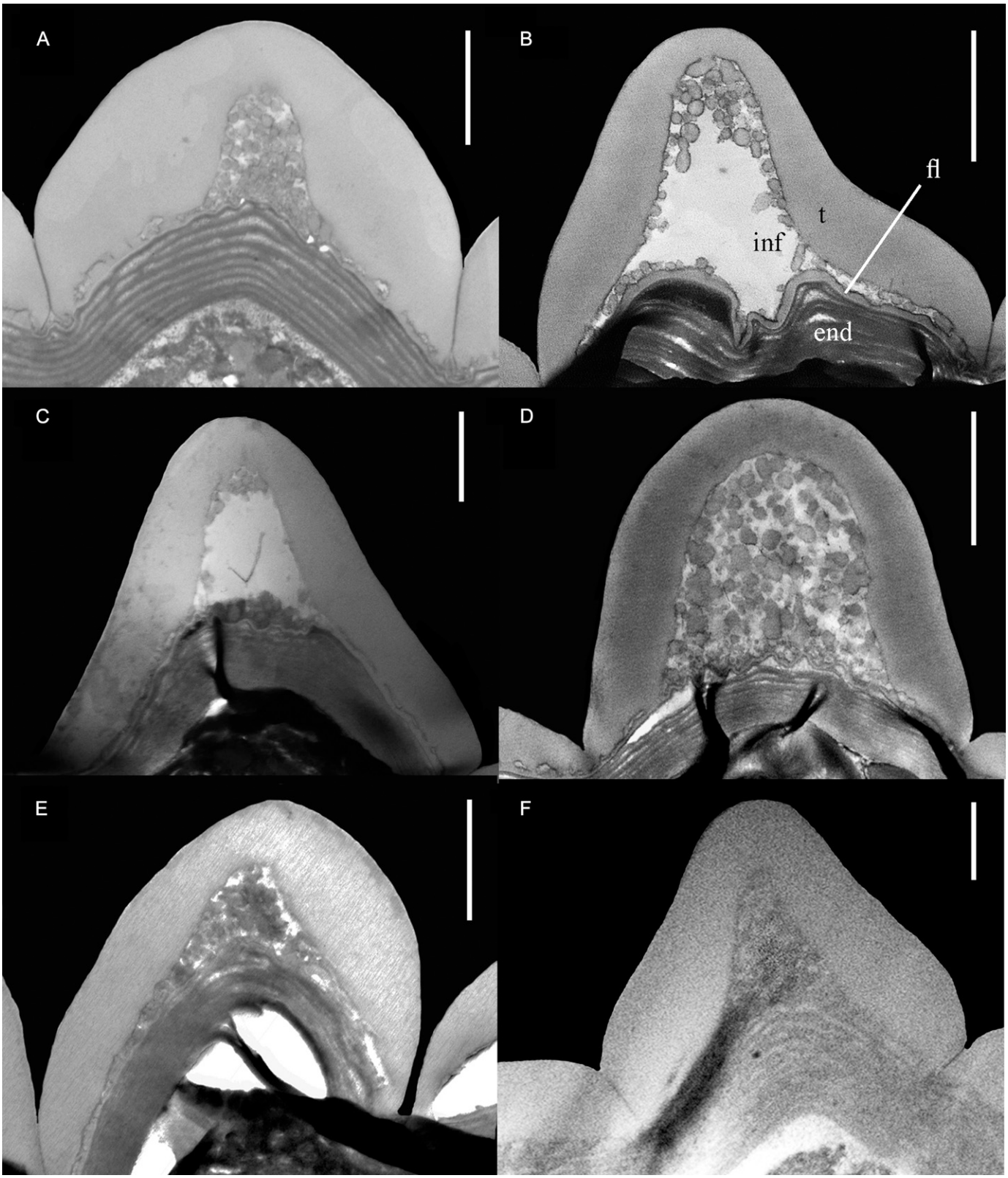

Fig. 2. Ultrastructure of *Ephedra* pollen grains in the plica region, t = tectum; inf = infratectum; fl = foot layer; end = endexine. (A) *E. foeminea* (B) *E. likiangensis* (C) *E. distachya* (D) *E. viridis* (E) *E. trifurca* (F) *E. nevadensis*. All species have a granular infratectum in the plica region; however the infratectum is in general not present between the plicae where the pseudosulci are found. In *E. foeminea* and *E. trifurca*, which have the ancestral pollen type, the infratectum makes up a comparatively small portion of the exine and there is a high density of granules. In *E. likiangensis, E. distachya*, *E. nevadensis* and *E. viridis,* which have the derived pollen type with, the infratectum typically makes up a larger portion of the exine compared to the ancestral type, and the granular infratectum is often more spacious. Scale bars = 1 μm.

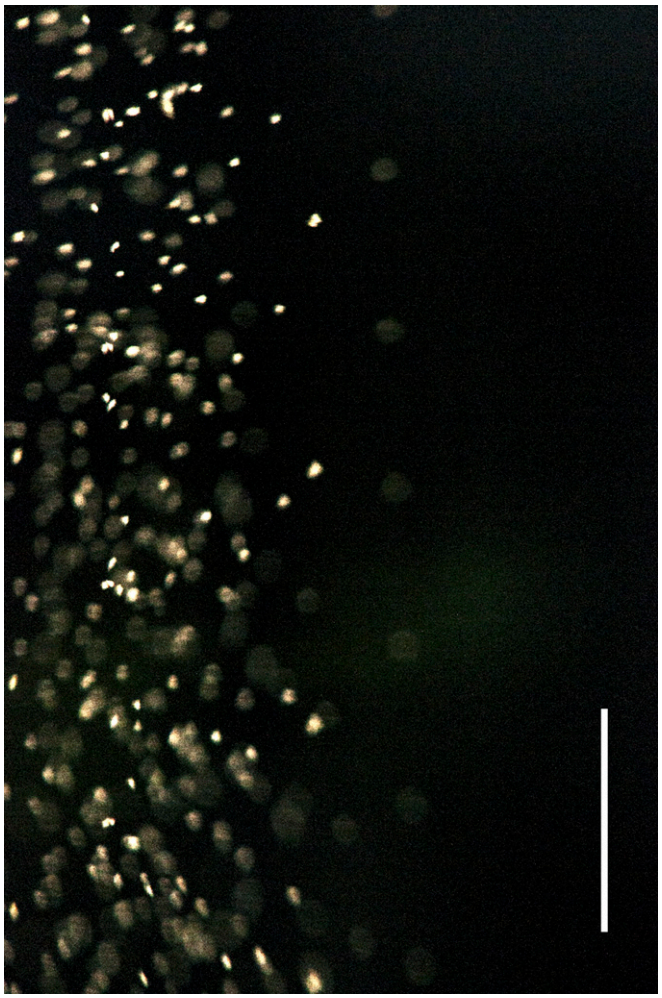

Fig. 3. Pollen grains of *Ephedra foeminea* falling through still air in stroboscopic illumination (40 flashes·min^{-1}) at a mean settling velocity of 10.18 (4.7–21.44) ± SD 4.10 cm·s^{-1}. The large variation in settling velocity among pollen grains (dispersal units) can be explained by the tendency of pollen grains of this species to form clumps. Scale bar = 5 mm.

real *E. foeminea* pollen. This protocol resulted in a deterministic model of pollen behavior for both lateral and polar views of the acceleration field, i.e., the consequences of stem oscillations, or variations in airflow patterns (mimicking wind gusts) and settling velocities were not considered.

***Pollen morphology*—**Anthetic microsporangiate structures were obtained from herbarium specimens of *E. distachya*, *E. foeminea*, *E. likiangensis* Florin, *E. nevadensis*, *E. trifurca*, and *E. viridis* Coville (Appendix 1). Pollen was taken from the herbarium specimen and studied without further preparation, since studies have shown that pretreatment in alcohol and/or acetolysis alters the size and morphology of *Ephedra* pollen significantly as compared with fresh pollen (K. Bolinder, personal observation; Kedves, 1987; Norbäck-Ivarsson, 2014). The best way to study natural variation in *Ephedra* pollen is therefore to use fresh or air-dried pollen. We suspect that the infraspecific variation and dimorphism of *Ephedra* pollen reported in the literature concerning "normal" pollen and a "variant" with curvy ridges (not furrows) is an artifact of specimen preparation (see also Norbäck-Ivarsson, 2014). To ensure consistency and accuracy of our results, we have consistently used air-dried pollen from herbarium sheets for our morphological studies.

Multiple accessions (specimens) were investigated for each species (Appendix 1), including the same accessions studied by Steeves and Barghoorn (1959). From each species, 53–217 fully developed and mature pollen grains were mounted on aluminum stubs, sputter coated with gold, and measured using SEM. As an estimate of the absolute size, the length of the equatorial axis, which in *Ephedra* is equal to the longest axis (Huynh, 1975; El-Ghazaly et al., 1998), was measured (online Appendix S4). A shape estimate was obtained by dividing the polar axis by the equatorial diameter (shape estimate = *P*/*E*) (online Appendix S4). The number of plicae was counted on the visible side of the pollen grain, and multiplied by two to obtain the total number of plicae for each pollen grain (online Appendix S4). To estimate the influence of phylogenetic signal on absolute size, *P*/*E*, and number of plicae, we compared the fit of three generalized least squares (GLS) models using the program R (R 3.1; R Development Core Team, 2014), code provided by Jeremy M. Beaulieu (based on Lavin et al., 2008). Phylogentic information for the six investigated species was obtained from Bolinder et al. (2014). The potential influence of phylogenetic signal was estimated by varying the branch length transformation parameter λ (Pagel, 1999) between 0 (no autocorrelation due to phylogeny) and 1 (variance changes perfectly with phylogeny). In the ordinary least squares (OLS) model, λ = 0. In the lambda-model, λ is estimated during model fitting and lies $0 < \lambda < 1$. In the model equivalent to Brownian motion (BM; Schluter et al., 1997), λ = 1. Model fit was assessed using the Akaike information criterion (AIC; Akaike, 1974). Having established that the best model is OLS and therefore that there is no phylogenetic signal in these data, a conventional ANOVA and Tukey's honestly significant difference (HSD) test in R 3.1. (R Development Core Team, 2014) was performed to compare absolute size, *P*/*E* ratios and number of plicae among all species and between species of different pollen types, i.e., with and without lateral branches on the pseudosulci. Using regression analyses in R 3.1 (R Development Core Team, 2014), we tested for any correlations between pollen morphology and U_t (using absolute size, *P*/*E*, and number of plicae as explanatory variables).

***Ultrastructure of six* Ephedra *species and* Welwitschia mirabilis—** Anthetic microsporangiate structures were obtained from herbarium specimens, or from cultivated specimens at the Bergius Botanic Garden and the greenhouses at Stockholm University (Appendix 1). Microsporangiophores from each species were prefixed in 2.5% glutaraldehyde in 0.1 M phosphate buffer (pH 7.4), postfixed in 2% OsO_4, dehydrated in a graded ethanol series, and embedded in TAAB 812 epoxy resin (Marivac, Halifax, Nova Scotia, Canada). Ultrathin sections were cut with a diamond knife in an ultra-microtome and collected on copper slot grids. Grids were double-stained with 2% uranyl acetate (45 min) and lead citrate (3 min), and fully developed pollen grains were examined using a JEOL JSM-7401F scanning transmission electron microscope (STEM) at 15 kV.

RESULTS

Aerodynamic features of* Ephedra foeminea—Terminal settling velocity*—Pollen grains of *E. foeminea* have a mean U_t of 10.18 (4.7–21.44) ± SD 4.10 cm·s^{-1}. Pollen grains of *W. mirabilis* were so adhesive that it was impossible to investigate U_t by stroboscopic photography.

Computer simulations of airflow and pollen grain motion— With an ambient windward airflow speed of 223.5 cm·s^{-1} (moving from left to right, Fig. 4), airflow speed decreased abruptly near the windward surface of the simulated ovule and pollination droplet with minor variations along this surface (Fig. 4B). Airflow speeds over the distal surface of the pollination droplet ranged between 50 and 90% of ambient airflow speed. Precipitous decreases in airflow speed occurred within the leeward airspace approximately one ovule diameter in width. Slightly beyond this distance (i.e., ≈5%), leeward airflow speeds ranged between 80 and 100% of ambient airflow speed. Airflow directions within grid cells around the ovule were predicted to be uniform in the general direction of downwind ambient airflow, i.e., from left to right (Fig. 4C). No significant regions of vector curl or vector divergence were observed in these simulations, although the pollination droplet extended within an airflow region predicted to behave with some degree of vorticity.

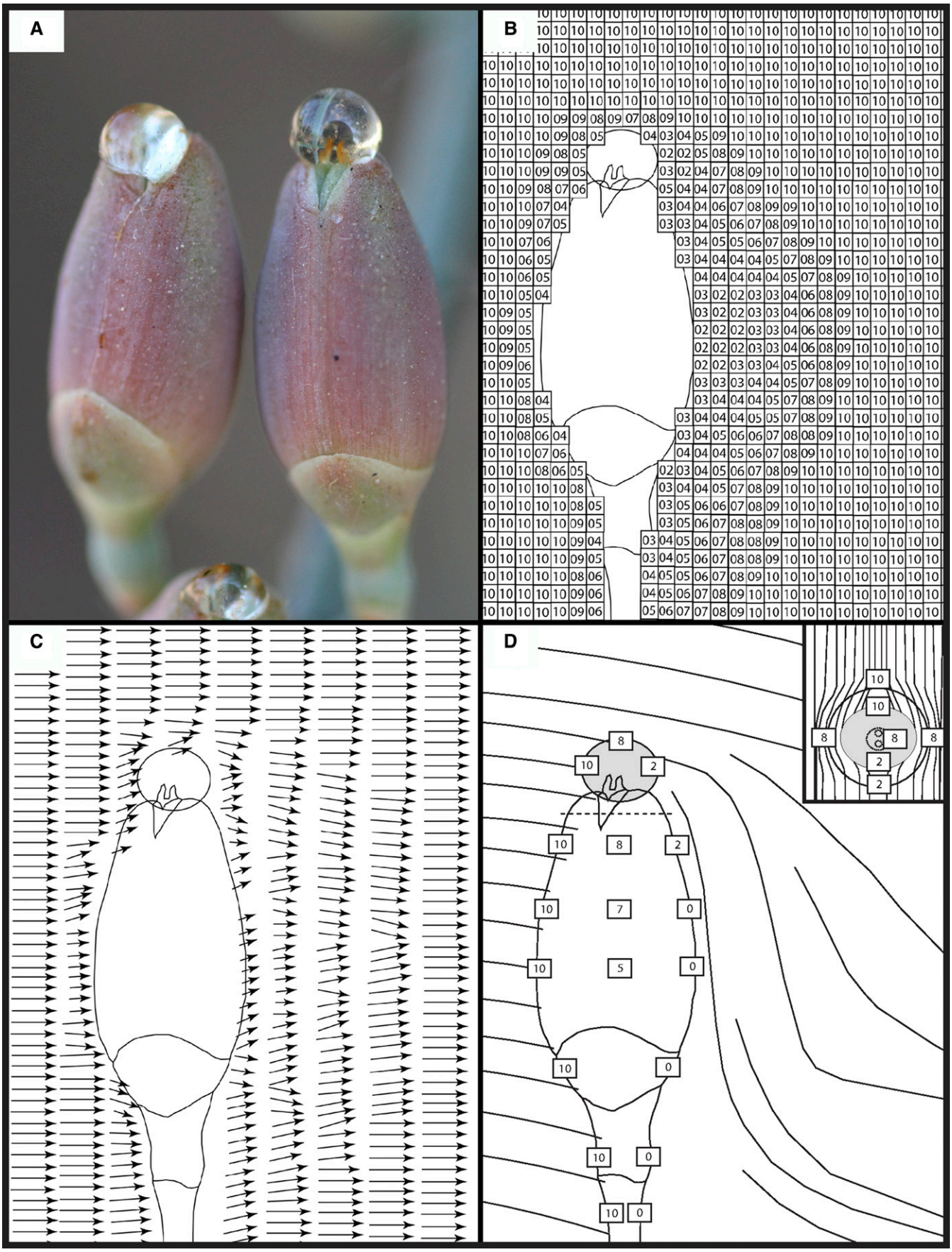
A
B
C
D

Impaction—Using the average dimensions and U_t of *E. foeminea* pollen grains, the airflow vector field created by and around the simulated ovule showed that this ovulate morphology had very little direct effect on pollen grain behavior other than to provide an obstruction to airflow. Pollen grain trajectories diverged from near parallel with the horizontal plane and arced downward under near the leeward vicinity of the ovule owing to the acceleration of gravity acting on their mass. With few exceptions, only those pollen trajectories that directly impacted windward surfaces were captured by the ovule or the pollination droplet (Fig. 4D). The exceptions to this general pattern were pollen grains captured via sedimentation by the more distal leeward surfaces of the pollination droplet or just beneath the droplet. This phenomenon was a consequence of the "tunneling" of airflow vectors passing under the lower curved surface of the droplet. Based on these observations, it was concluded that the morphology of an average *E. foeminea* ovule is not particularly well adapted for wind pollination, since virtually any obstruction to airflow corresponding to a prolate spheroid of its size and eccentricity would be as efficient at capturing airborne pollen as the model ovule tested in this study.

***Pollen properties*—**Pollen grains of *Ephedra* are polyplicate, and psilate on the plicae (Fig. 1). Their absolute size (equatorial diameter), *P*/*E* ratio, and number of plicae vary among species and to some extent also within species (Table 1). The terminology follows Punt et al. (2007), except regarding the furrows between plicae, which we call pseudosulci (see the introduction).

For these six species, there is no autocorrelation due to phylogenetic distance in the pollen traits here investigated. Pollen size (as gauged by the equatorial diameter): BM: ΔAIC = 2.58, lambda: ΔAIC = 2.00, OLS: ΔAIC = 0, pollen shape (*P*/*E*): BM: ΔAIC = 1.36, lambda: ΔAIC = 2.00, OLS: ΔAIC = 0, the number of plicae: BM: ΔAIC = 2.77, lambda: ΔAIC = 2.00, OLS: ΔAIC = 0. λ is a robust statistical index with low rates of type I error (Freckleton et al., 2002). We therefore assumed no phylogenetic autocorrelation between the groups (accept model OLS as the best model) and used a conventional one-way ANOVA of independent groups and Tukey's HSD to compare pollen size, pollen shape, and number of plicae among the different species as well as among the pollen of the two types, i.e., with and without lateral branches on the pseudosulci.

The absolute size (equatorial diameter) varies significantly between the six species ($F_{5, 742} = 220.4$, $P < 0.001$) (Fig. 5A). Pollen of the ancestral pollen type (with unbranched pseudosulci), i.e., *E. foeminea* and *E. trifurca*, are significantly smaller than pollen of the derived type (with branched pseudosulci) $F_{1, 746} = 562.8$, $P < 0.001$ (Fig. 5B). The shape estimate, *P*/*E* ratio, varies significantly between the species investigated ($F_{5, 742} = 10.5$, $P < 0.001$) (Fig. 5C) but not between species of different pollen types ($F_{1, 746} = 0.23$, $P = 0.63$) (Fig. 5D). The number of plicae varies significantly between the six different species ($F_{5, 742} = 645.6$, $P < 0.001$), only *E. distachya* and *E. viridis* (Tukey HSD; diff = 9.55, $P = 0.97$) and *E. trifurca* and *E. foeminea* (Tukey HSD; diff = 0.48 $P = 0.25$) do not differ significantly from each other (Fig. 5E). Pollen of the ancestral type (with unbranched pseudosulci) have a significantly higher number of plicae ($F_{1, 746} = 1867$ $P < 0.001$), than that of the derived type (with branched pseudosulci) (Fig. 5F).

Between the three taxa, for which terminal settling velocity is known (Table 2), there is no correlation between absolute size ($r_s = 0.43$, $P = 0.36$), *P*/*E* ratio ($r_s = 0.72$, $P = 0.25$), or number of plicae ($r_s = 0.14$, $P = 0.45$).

***Ultrastructure of six* Ephedra *species and* Welwitschia mirabilis—**The ectexine consists of a tectum, which is homogenous in texture, and an infratectum, which is granular. The foot layer is thin and adnate to the endexine. The structure of the endexine is lamellar (Fig. 2).

Ephedra foeminea—The tectum is distinctly thinner at the top of the plicae (0.57 ± 0.23 μm in studied pollen) and thicker at its sides and bases (1.20 ± 0.38 μm). The infractectum is granular with a high density of small granules of equal size. The granular infratectum constitutes only a small fraction of the plicae (Fig. 2A).

Ephedra likiangensis—The tectum is thin (0.49 ± 0.10 μm in studied pollen) and almost uniform in thickness over the plicae. The infratectum is large and spacious with small amounts of granules of equal size (Fig. 2B).

Ephedra distachya—The tectum is thin (0.73 ± 0.14 μm in studied pollen) and uniform in thickness over the plicae. The infratectum is broad and spacious with small amounts of granules of equal size (Fig. 2C).

Ephedra viridis—The tectum is thin (0.58 ± 0.08 μm in studied pollen) and uniform in thickness over the plicae. The infratectum is very large and spacious with granules of equal size (Fig. 2D).

Ephedra trifurca—The tectum is relatively thick (0.67 ± 0.09 μm in studied pollen). It is slightly thinner at the top of the plicae and thicker at its sides and base. The infractectum is granular with a high density of small granules of equal size (Fig. 2E).

Ephedra nevadensis—The tectum is relatively thin (0.86 ± 0.20 μm in studied pollen). It is slightly thinner at the top of the plicae and thicker at its sides and base. The infratectum is broad and granular with small granules of equal size (Fig. 2F).

←

Fig. 4. Computer simulated behavior of pollen grains around an ovule of *Ephedra foeminea* based on an acceleration field generated around an ovule by an ambient airflow speed of 223.5 cm·s^{-1} (moving from left to right). The acceleration field around a representative ovule was simulated based on estimates of the speed and direction (B and C, respectively) of air passing through a Cartesian coordinate system composed of 945 grid cells. (A) Photo of a pair of typical ovules with pollination droplets. (B) Airflow magnitudes around an ovule normalized with respect to the ambient airflow speed (10 = 223.5 cm·s^{-1}). (C) Airflow direction as indicated by arrows. (D) Predicted inflight trajectories of *E. foeminea* pollen grains in the acceleration field in lateral and polar view (upper right). The dashed line in the lateral view represents the approximate level of the view shown in the polar simulation. Pollination droplet is shaded gray. Numbers of pollen grains (of a total of 500 pollen grains released upwind) estimated to impact the surfaces of the ovule and the pollination droplet are shown in boxes.

TABLE 1. Investigated pollen properties for the six different *Ephedra* species.

Species	Mean (± SD) length of polar axis (μm)	Mean (± SD) equatorial diameter (μm)	Mean (± SD) *P*/*E* ratio	Mean no. (± SD) of plicae (n ± SD)	Plicae merge at the tips	Branched pseudosulci
E. distachya	19.97 ± 1.73	49.58 ± 3.60	0.40 ± 0.06	6.67 ± 1.27	yes	yes
E. foeminea	18.06 ± 2.29	42.18 ± 3.97	0.43 ± 0.048	15.75 ± 2.61	yes	no
E. likiangensis	20.28 ± 2.44	46.92 ± 5.02	0.44 ± 0.06	13.00 ± 2.25	yes	yes
E. nevadensis	24.73 ± 2.29	60.07 ± 6.07	0.42 ± 0.07	8.00 ± 1.36	yes	yes
E. trifurca	18.44 ± 2.44	44.09 ± 5.11	0.42 ± 0.08	16.22 ± 2.52	yes	no
E. viridis	24.38 ± 2.70	54.11 ± 5.16	0.45 ± 0.043	6.87 ± 1.21	yes	yes

Note: Properties are for the pollen grains investigated here; additional intraspecific variation may be present.

Welwitschia mirabilis—Pollen grains of *Welwitschia mirabilis* differ from those of *Ephedra* in that they are monosulcate (Zavada and Gabarayeva, 1991; Carafa et al., 1996) (Fig. 6A, B). The tectum is thick (0.86 ± 0.07 μm in studied pollen) and largely uniform in thickness over the plicae (Fig. 6B, C). The infratectum is densely granular and restricted to a small space at the center of each plica, a narrow area between plicae, and the aperture region (Fig. 6B, C).

DISCUSSION

Settling velocity—Aerodynamic properties of pollen grains are known to vary greatly among plant groups (Di-Giovanni et al., 1995). A correlation between small size and slow settling velocity of pollen grains has been shown (Hall and Walter, 2011). However, because large dense pollen grains generally have a larger forward momentum, their inflight trajectories can more easily diverge from air streamlines and are thus to a larger degree affected by the acceleration fields generated by and around pollen receptive organs (Whitehead, 1983). Thus, wind-pollinated plants experience a trade-off between having small and light pollen that can travel long distances and having large and dense pollen that are more easily trapped by ovulate reproductive structures (Whitehead, 1983). Therefore, it is not surprising that the settling velocity of a wind-pollinated plant can in some cases exceed that of an insect-pollinated plant, as shown by Hall and Walter (2011). Consequently, the terminal settling velocity of pollen taken in isolation does not provide sufficient evidence to affirm the presence of one pollination syndrome over another, especially not when comparing distantly related taxa.

In the current study, we compared the terminal settling velocities of closely related taxa with presumably different pollination syndromes, as judged from field studies (Bolinder et al., 2014) and from wind-tunnel experiments (Niklas et al., 1986; Niklas and Kerchner, 1986; Niklas and Buchmann, 1987; Buchmann et al., 1989). Even though only a few species of *Ephedra* have been investigated experimentally, it is nevertheless obvious that the variation among species is substantial. Here we show that the pollen grains of the entomophilous *Ephedra foeminea* have a higher terminal settling velocity than pollen grains of the previously studied *E. nevadensis* and *E. trifurca* (Table 2), which are purported to be anemophilous (Niklas et al., 1986; Niklas and Kerchner, 1986; Niklas and Buchmann, 1987; Buchmann et al., 1989). Thus, our data indicate that the pollen grains of *E. foeminea* descend faster and are less likely to travel great distances under the same atmospheric conditions than are the pollen grains of *E. nevadensis* or *E. trifurca*. The difference between *E. foeminea* and the other investigated species may be even greater than reported here, since the pollen grains of *E. foeminea* were stored in a refrigerator until the time of experimentation and the resulting dehydration probably resulted in an underestimation of their terminal settling velocity (Hall and Walter, 2011).

The observed differences in aerodynamic properties of pollen grains reflect differences in pollination biology among studied taxa. In general, the terminal settling velocities of wind-pollinated species are noticeably lower. For example, *Pinus sylvestris* L. has a U_t of 2.5 cm·s^{-1} (Niklas, 1982), which enables pollen to travel considerable distances by air. In contrast, pollen grains of insect-pollinated taxa generally have low dispersability because of their higher U_t. The U_t of insect-pollinated taxa is rarely measured but, for example, pollen of the insect-pollinated species *Cabomba caroliniana* A.Gray has a U_t of 19.5 cm·s^{-1} (Osborn et al., 1991). Although the difference in U_t between the various species of *Ephedra* are less dramatic compared with that between *P. sylvestris* and *C. caroliniana*, we nevertheless judge these differences apparent and significant, as well as congruent with previous studies of the pollination biology of this genus. Early interpretations (Porsch, 1910) and recent field experimentation (Bolinder et al., 2014) showed that *E. foeminea* is insect-pollinated, which is consistent with the aerodynamic features of the pollen grains as estimated here. In contrast, most other species of *Ephedra* (including *E. distachya*, *E. nevadenesis*, and *E. trifuca*) are interpreted as anemophilous (Niklas et al., 1986; Niklas and Kerchner, 1986; Niklas and Buchmann, 1987; Buchmann et al., 1989; Bolinder et al., 2014). Based on field experimentation, Bolinder et al. (2014) show that *E. distachya* is wind-pollinated and that its pollen grains travel significantly greater distances than do pollen grains of *E. foeminea*. This indicates (although not explicitly tested) that *E. distachya* pollen has slower settling velocity than pollen of *E. foeminea.*

Insect pollination is probably the ancestral pollination mode in *Ephedra* and possibly within the Gnetales as a whole. It is present in *Gnetum* L. (Kato et al., 1995), *Welwitschia* (Hooker, 1863; Baines, 1864; Wetschnig and Depish, 1999), and retained in *Ephedra foeminea*, which is the sister species of all other species of *Ephedra* (Rydin and Korall, 2009). Pollen grains of *Welwitschia* are similar to those of *Ephedra* in their polyplicate exine, but they differ in that *Welwitschia* grains have a single, broad, sulcus, which extends over the entire pollen grain along the equatorial axis (Fig. 6A, B). Although pollen of *Welwitschia* was included in the current study for comparison, its settling velocity could not be measured as a consequence of their cohesiveness. We nevertheless expect the settling velocity of *Welwitschia* pollen to be high, and thus its flight capability to be low (see further below).

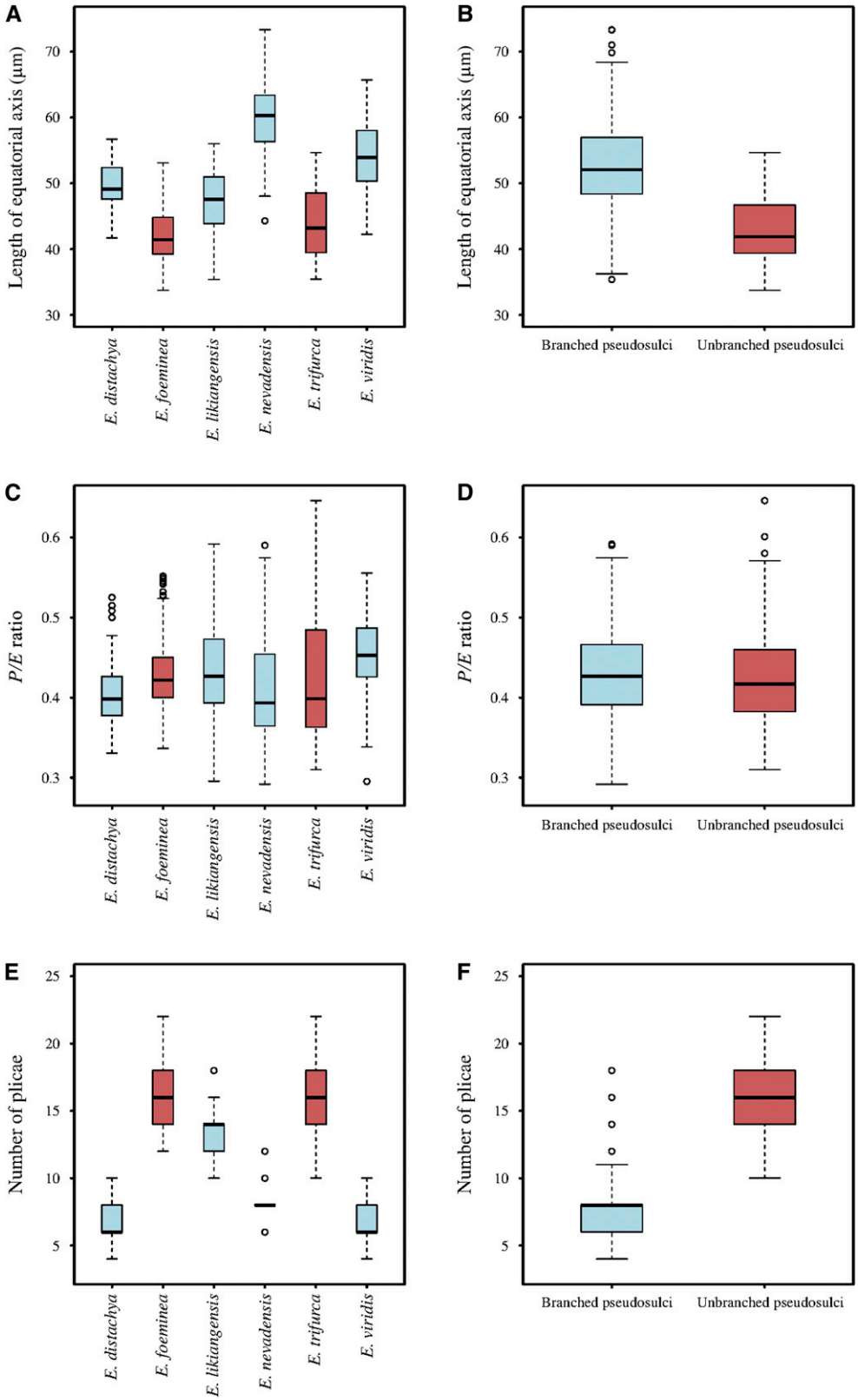

Fig. 5. Boxplots showing differences between the six species investigated in (A) absolute size (length of equatorial axis), (C) *P*/*E* ratio and (E) number of plicae. Species with unbranched pseudosulci are in red, species with branched pseudosulci in blue. Differences between pollen of the ancestral pollen type, with unbranched pseudosulci, (shown in red) and pollen of the derived pollen type branched pseudosulci (shown in blue) in (B) absolute size, (D) *P*/*E* ratio, and (F) number of plicae.

TABLE 2. The settling velocity and pollination syndrome of *Ephedra foeminea*, *E. nevadensis*, and *E. trifurca*.

Feature	*E. foeminea*	*E. nevadensis*	*E. trifurca*
Mean settling velocity ± SD (min.–max.)	10.18 (4.7–21.44) ± 4.10 [a]	3.6 (2.8–4.0) ± 0.9 [b]	6.1 (4.0–6.5) ± 2.0 [b]
Pollination syndrome	Entomophilous [c]	Anemophilous[b,d,e,f]	Anemophilous[b,d,e,f]

[a]Note the large span between minimum and maximum settling velocity. Pollen grains dispersed as clumps have a larger settling velocity than those dispersed as singletons.

Source notes: [b] Niklas and Buchmann, 1987; [c] Bolinder et al., 2014; [d] Buchmannet al., 1989; [e] Niklas et al., 1986; [f] Niklas and Kerchner, 1986.

Pollen reception—It is obvious that, to accomplish successful fertilization, pollen grains must be transported to the ovulate organs. However, pollen grains must also be effectively caught by reproductively receptive organ parts. In most gymnosperms, pollen is received by a pollination drop (produced by cellular degradation in the distal part of the nucellus) that is secreted through the micropyle (Chamberlain, 1935; Takaso, 1990). In wind-pollinated taxa, the surface of the droplet is the receptive area. However, the aerodynamics around this receptive surface is not governed exclusively by the airflow patterns it generates in isolation. The acceleration field around the pollination droplet is additionally influenced by the aerodynamics of the ovule, to which it is attached, as well as other neighboring structures (Niklas, 1985). For example, the airflow created around the ovules and stems of the wind-pollinated *E. trifurca* generates a unique aerodynamic region around the ovules, in which air currents are canalized toward the micropylar tube and the pollination drop (Niklas et al., 1986). Conspecific pollen grains or pollen grains of the same size and density are the most likely to end up in the vicinity of the pollination droplet and thus fertilize the ovule (Niklas and Kerchner, 1986; Buchmann et al., 1989). In *E. trifurca*, this system is so well defined that it can sort out conspecific pollen grains from those of the sympatric and closely related *E. nevadensis* (Niklas and Buchmann, 1987).

In contrast, in entomophilous taxa, the aerodynamic patterns created around ovulate organs are of less importance since pollen is delivered to the pollination drop by insect vectors. Therefore, it is not surprising that our simulations show that the ovules of *E. foeminea* fail to create an airflow pattern that increases the probability of pollen capture by directing currents toward the pollination drop (Fig. 4). The failure to detect any evidence of aerodynamic specialization in the ovules of this species does, in itself, not preclude the possibility that airborne pollen can be captured by *E. foeminea* ovules, because any insect-pollinated plant with emergent reproductively receptive surfaces (such as a pollination droplet) can capture airborne pollen. However, the evidence presented here demonstrates that anemophily is extremely inefficient in *E. foeminea*, which is consistent with the fact that only a minor fraction of its ovules are fertilized when insects are experimentally denied access to ovules (Bolinder et al., 2014).

Differences among taxa—There are considerable differences in aerodynamic properties among the species in *Ephedra*, which reflect variation in pollination syndrome in the clade. It is however less clear how the functional differences are accomplished. Gross morphological divergence of ovulate structures is limited in *Ephedra* (Ickert-Bond and Wojciechowski, 2004; Rydin et al., 2010) but, as shown by simulations of airflow around ovules (the current study, Niklas et al., 1986; Niklas and Kerchner, 1986; Niklas and Buchmann, 1987; Buchmann et al., 1989), seemingly small differences in pollen and/or ovule morphology may result in profoundly different functional properties. Similarly, the overall morphological distinction between pollen types in *Ephedra* (and *Welwitschia*) is limited. For example, the anemophilous *E. trifurca* has retained the ancestral pollen type, and its pollen does not differ substantially in size or number of plicae from pollen of *E. foeminea* (Fig. 5A, E), but has nevertheless a slower settling velocity than pollen of *E. foeminea* (Table 2).

Clearly when considering the "size" of a dispersal unit, we must also ask whether the unit is a single pollen grain or a clump of grains. For example, there is substantial variation in the U_t among pollen grains of *E. foeminea* (Table 2). This can be explained by a tendency of its pollen to aggregate into larger clumps, the size of which affects U_t and thus dispersal distance (Hall and Walter, 2011). A similar tendency is also obvious in the entomophilous *Welwitschia* (Hesse, 1984; present study). In contrast, in the anemophilous *E. distachya,* pollen disperses as singletons (Bolinder et al., 2014). It is worth noting that the Gnetales are reported to lack pollenkitt (Hesse, 1984), and the means by which the pollen grains of *E. foeminea* and *Welwitschia* aggregate are currently unknown.

Further, a critical consideration when comparing the aerodynamic properties of the pollen within this clade is that pollen size and bulk density have equal consequences on the terminal settling velocity. Thus, a small but dense pollen grain can settle as rapidly as a larger but less dense pollen grain. The interplay between these two variables may explain why the pollen of *E. foeminea* has the fastest U_t (Table 2), and yet, together with *E. trifurca*, it is significantly smaller than the pollen grains of other investigated taxa (Fig. 5A, B). Indeed, among the *Ephedra* species investigated in this study, U_t is not correlated with pollen size or shape, nor with the number of plicae, such that the observed substantial differences in U_t implicate bulk density as the critical variable of interest. The density of cell protoplasm does not vary among closely related plant species (Niklas, 1985), but properties of the pollen wall may result in variation in the overall, bulk density of pollen grains of the same size.

The pollen wall in *Ephedra* is composed of a compact tectum, a granular infratectum and a uniform lamellate endexine (Gullvåg, 1966; Van Campo and Lugardon, 1973; Hesse, 1984; Zavada, 1984; Kurmann, 1992; Rowley, 1995; El-Ghazaly et al., 1998; Tekleva and Krassilov, 2009). Our studies demonstrate differences among species regarding the thickness of the tectum and the density of the granular infratectum. The pollen exine of *E. foeminea* is to a larger extent composed of a dense tectum, and the granular infratectum contains a higher density of granules compared to the other species (Fig. 2A) (see also Hesse, 1984). Conceivably, these features are ancestral in the Gnetales. The tectum is thick also in *Welwitschia* pollen (Fig. 6), and more or less uniform in thickness throughout the plicae

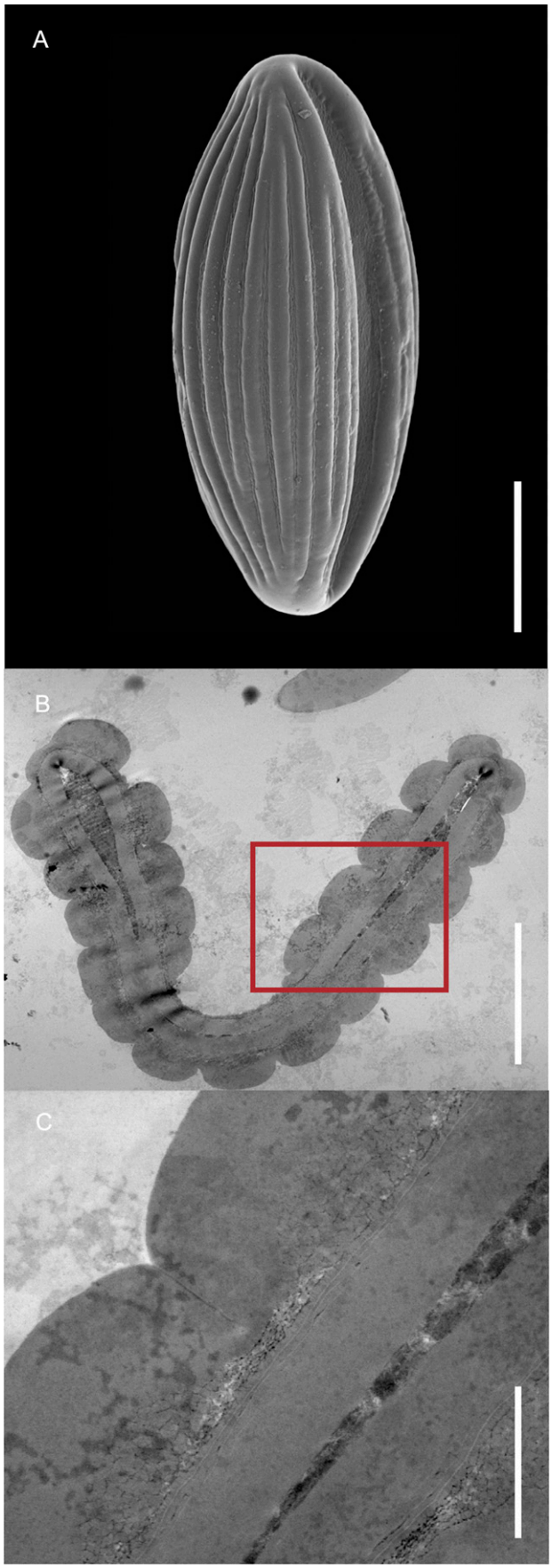

(Fig. 6, see also Tekleva and Krassilov, 2009). In addition, the granular space of the infratectum is extremely dense (Fig. 6). We believe that the U_t of *Welwitschia* grains would have been very fast, had it been possible to measure this feature for an individual pollen grain. These findings and interpretations are in agreement with Wetschnig and Depish (1999), who reported that *Welwitschia* pollen is capable of traveling only short distances by air.

In contrast, the exine of *E. distachya* is composed of a thinner tectum and a more spacious granular infratectum with a low density of granules (Fig. 2C) (see also Van Campo and Lugardon, 1973; Kurmann, 1992; El-Ghazaly et al., 1998). The same is true for most other (presumably anemophilous) taxa studied here, as well as for previously studied *Ephedra* species: *E. americana* (Hesse, 1984), *E. californica* (Zavada, 1984), *E. foliata* (Rowley, 1995; El-Ghazaly and Rowley, 1997), and *E. monosperma* (Gullvåg, 1966; Tekleva and Krassilov, 2009). This pattern with a denser exine and a larger tectum/nexine ratio for animal-pollinated taxa than for wind-pollinated taxa has also been shown for angiosperms, e.g., in Asteraceae (Bolick, 1990) and Cabombaceae (Osborn et al., 1991).

Pollen grains of *E. trifurca* are of the ancestral type (Fig. 1E) and have, like pollen of *E. foeminea,* a thick tectum and a dense granular infratectum (Fig. 2E) and, consequently, a relatively fast settling velocity (Table 1). However, the pollen grains of *E. trifurca* are nonadhesive and the settling velocity of single grains is lower than that of *E. foeminea* (Table 1). Further, unlike the ovulate structures of *E. foeminea*, the ovules of *E. trifurca* effectively trap conspecific pollen grains (Niklas et al., 1986; Niklas and Kerchner, 1986; Niklas and Buchmann, 1987; Buchmann et al., 1989), and successful wind pollination is accomplished although the pollen grains have retained many features of its entomophilous ancestors.

Evolutionary remarks— An evolutionary shift in *Ephedra*, from insect pollination to wind pollination, has been hypothesized to have occurred before the diversification of the core clade (Bolinder et al., 2014). The current study presents evidence that adaptations for anemophily in the genus extend to the microgametophytic level. Pollen grains of anemophilous taxa have a better flight ability than those of the entomophilous sister species of the remaining genus (*E. foeminea*), and the slower settling velocities of pollen of anemophilous taxa are accomplished by a thinner tectum, and generally also a more sparsely granulate infratectum. It is possible that these differences between entomophilous and anemophilous members of the Gnetales can be used to assess the pollination syndromes of fossil plants that produce so called "ephedroid" pollen. This type of pollen fluctuate in abundance in geological time (Crane, 1986). After a decline in the Jurassic (Crane, 1986), ephedroid pollen increases in abundance in the Early Cretaceous and decreases toward the latter part of the Cretaceous (Crane and Lidgard, 1989), but appears to have become more common

Fig. 6. Pollen morphology and ultrastructure of *Welwitschia mirabilis*. (A) SEM photo of a pollen grain. Note high number of plicae and presence of a broad sulcus along the equatorial axis. Scale bar = 15 µm. (B) Ultrastructure of the pollen wall in the sulcus and the plica region. Scale bar = 5 µm. (C) Close up of the ultrastructure of two plicae. The tectum is thick and largely uniform in thickness over the plica. The infratectum is densely granular and present also between the plicae. The endexine is thick and laminated. Scale bar = 1 µm.

again in the late Paleogene, even though no quantitative studies have been undertaken for this period. Although it is far from clear that all striate Cretaceous pollen referred to as "ephedroids" were produced by a single group of species, the affinity to Gnetales or extinct relatives of individual grains can be assessed using ultrastructural information from the pollen wall (see also discussion in Friis et al., 2011). When the ultrastructure of Mesozoic ephedroid palynomorphs is known and described (Trevisan, 1980; Osborn et al., 1993), it is always of the ancestral type with a thick tectum and dense infratectum. Based on the available information, we speculate that some or even most of the Cretaceous "ephedroid" pollen was produced by insect-pollinated plants. Further, our results indicate that if ovulate structures are three-dimensionally preserved and found in association with pollen (see e.g., Rydin et al., 2004), it may be possible to simulate pollen capture efficiency to assess the pollination biology of these extinct plants.

LITERATURE CITED

Ackerman, J. 2000. Abiotic pollen and pollination: Ecological, functional, and evolutionary perspectives. *Plant Systematics and Evolution* 222: 167–185.

Akaike, H. 1974. A new look at the statistical model identification. *IEEE Transactions on Automatic Control* 19: 716–723.

Baines, T. 1864. Explorations in South-West Africa: Being an account of a journey in the years 1861 and 1862 from Walvisch Bay, on the western coast, to Lake Ngami and the Victoria Falls. Longman Green Longman Roberts & Green, London, UK.

Bharadwaj, D. 1963. Pollen grains of *Ephedra* and *Welwitschia* and their probable fossil relatives. *Memoirs of the Indian Botanical Society* 4: 125–135.

Bino, R. J., A. Dafni, and A. D. J. Meeuse. 1984. Entomophily in the dioecious gymnosperm *Ephedra aphylla* Forsk. (=*E. alte* C.A. Mey.), with some notes on *E. campylopoda* C.A. Mey. I. Aspects of the entomophilous syndrome. *Proceedings of the Koninklijke Nederlandse Akademie van Wetenschappen, C, Biological and Medical Sciences* 87: 1–13.

Bolick, M. R. 1990. The pollen surface in wind-pollination with emphasis on the Compositae. *In* M. Hesse and F. Ehrendorfer [eds.], Morphology, development, and systematic relevance of pollen and spores, 39–51. Springer-Verlag, Vienna, Austria.

Bolinder, K., A. M. Humphreys, J. Ehrlén, R. Alexandersson, S. M. Ickert-Bond, and C. Rydin. 2014. Pollination mechanisms in the ancient gymnosperm clade *Ephedra* (Gnetales). *In* K. Bolinder [ed.], Pollination in *Ephedra* (Gnetales), 29–45. Licentiate thesis, Stockholm University, Stockholm, Sweden.

Buchmann, S. L., M. K. O'Rourke, and K. J. Niklas. 1989. Aerodynamics of *Ephedra trifurca*. III. Selective pollen capture by pollination droplets. *Botanical Gazette* 150: 122–131.

Carafa, A. M., R. Ponzi, and F. Pizzolongo. 1996. Some aspects of microsporogenesis of *Welwitschia mirabilis* Hook. *Plant Biosystems* 130: 557–565.

Chamberlain, C. J. 1935. Gymnosperms: Structure and evolution. University of Chicago Press, Chicago, Illinois, USA.

Crane, P. R. 1986. Form and function in wind dispersed pollen. *In* S. Blackmore and I. K. Ferguson [eds.], Pollen and spores: Form and function, 179–202. Academic Press, Orlando, Florida, USA.

Crane, P. R., and S. Lidgard. 1989. Angiosperm diversification and palaeolatitudinal gradients in Cretaceous floristic diversity. *Science* 246: 675–678.

Cresswell, J. E., J. Krick, M. Patrick, A., and M. Lahoubi. 2010. The aerodynamics and efficiency of wind pollination in grasses. *Functional Ecology* 24: 706–713.

Culley, T. M., S. G. Weller, and A. K. Sakai. 2002. The evolution of wind pollination in angiosperms. *Trends in Ecology & Evolution* 17: 361–369.

Di-Giovanni, F., P. Kevan, and M. Nasr. 1995. The variability in settling velocities of some pollen and spores. *Grana* 34: 39–44.

El-Ghazaly, G., and J. R. Rowley. 1997. Pollen wall of *Ephedra foliata. Palynology* 21: 7–18.

El-Ghazaly, G., J. R. Rowley, and M. Hesse. 1998. Polarity, aperture condition and germination in pollen grains of *Ephedra* (Gnetales). *Plant Systematics and Evolution* 213: 217–231.

Erdtman, G. 1952. Pollen morphology and plant taxonomy: An introduction to palynology. Almqvist and Wiksell, Stockholm, Sweden.

Faegri, K., and L. van der Pijl. 1979. The principles of pollination ecology. Pergamon Press, Oxford, UK.

Ferguson, I. K., and J. J. Skvarla. 1982. Pollen morphology in relation to pollinators in Papilionoideae (Leguminosae). *Botanical Journal of the Linnean Society* 84: 183–193.

Freckleton, R. P., P. H. Harvey, and M. Pagel. 2002. Phylogenetic analysis and comparative data: A test and review of evidence. *American Naturalist* 160: 712–726.

Friedman, J., and S. C. H. Barrett. 2008. A phylogenetic analysis of the evolution of wind pollination in the angiosperms. *International Journal of Plant Sciences* 169: 49–58.

Friis, E. M., P. R. Crane, and K. R. Pedersen. 2011. Early flowers and angiosperm evolution. Cambridge University Press, New York, New York, USA.

Grayum, M. H. 1986. Correlations between pollination biology and pollen morphology in the Araceae, with some implications for angiosperm evolution. *In* S. Blackmore and I. K. Ferguson [eds.], Pollen and spores: Form and function, 313–327. Academic Press, Orlando, Florida, USA.

Gullvåg, B. M. 1966. The fine structure of some gymnosperm pollen walls. *Grana* 6: 435–475.

Hall, J. A., and G. H. Walter. 2011. Does pollen aerodynamics correlate with pollination vector? Pollen settling velocity as a test for wind versus insect pollination among cycads (Gymnospermae: Cycadaceae: Zamiaceae). *Biological Journal of the Linnean Society* 104: 75–92.

Hesse, M. 1981. The fine structure of the exine in relation to the stickiness of angiosperm pollen. *Review of Palaeobotany and Palynology* 35: 81–92.

Hesse, M. 1984. Pollenkitt is lacking in Gnetatae: *Ephedra* and *Welwitschia*; further proof for its restriction to the angiosperms. *Plant Systematics and Evolution* 144: 9–16.

Hooker, J. D. 1863. On *Welwitschia*, a new genus of Gnetaceae. *Transactions of the Linnean Society of London* 24: 1–48.

Huynh, K.-L. 1975. Le probléme de la polarité du pollen d'*Ephedra. Pollen et Spores* 16: 469–474.

Ickert-Bond, S. M., J. J. Skvarla, and W. F. Chissoe. 2003. Pollen dimorphism in *Ephedra* L. (Ephedraceae). *Review of Palaeobotany and Palynology* 124: 325–334.

Ickert-Bond, S. M., and M. F. Wojciechowski. 2004. Phylogenetic relationships in *Ephedra* (Gnetales): Evidence from nuclear and chloroplast DNA sequence data. *Systematic Botany* 29: 834–849.

Kato, M., T. Inoue, and T. Nagamitsu. 1995. Pollination biology of *Gnetum* (Gnetaceae) in a lowland mixed dipterocarp forest in Sarawak. *American Journal of Botany* 82: 862–868.

Kedves, M. 1987. LM and EM studies on pollen grains of recent *Welwitschia mirabilis* Hook. and *Ephedra* species. *Acta Botanica Hungarica* 33: 81–103.

Kubitzki, K. 1990. Ephedraceae. *In* K. Kubitzki [ed.], The families and genera of vascular plants. I. Pteridophytes and gymnosperms, 379–382. Springer Verlag, Berlin, Germany.

Kurmann, M. H. 1992. Exine stratification in extant gymnosperms: A review of published transmission electron micrographs. *Kew Bulletin* 47: 25–39.

Kurmann, M. H., and M. S. Zavada. 1994. Pollen morphological diversity in extant and fossil gymnosperms. *In* M. H. Kurmann and J. A. Doyle [eds.], Ultrastructure of fossil spores and pollen, 123–137. Royal Botanic Gradens, Kew, London, UK.

Land, W. 1907. Fertilization and embryogeny in *Ephedra trifurca. Botanical Gazette* 44: 273–292.

LAVIN, S. R., W. H. KARASOV, A. R. IVES, K. M. MIDDLETON, AND T. GARLAND JR. 2008. Morphometrics of the avian small intestine compared with that of nonflying mammals: A phylogenetic approach. *Physiological and Biochemical Zoology* 81: 526–550.

MEEUSE, A. D. J., A. H. DE MEIJER, O. W. P. MOHR, AND S. M. WELLINGA. 1990. Entomophily in the dioecious gymnosperm *Ephedra aphylla* Forsk. (=*E. alte* C.A. Mey.), with some notes on *Ephedra campylopoda* C.A.Mey. III. Further anthecological studies and relative importance of entomophily. *Israel Journal of Botany* 39: 113–123.

NIKLAS, K. J. 1982. Simulated and empiric wind pollination patterns of conifer ovulate cones. *Proceedings of the National Academy of Sciences, USA* 79: 510–514.

NIKLAS, K. J. 1985. The aerodynamics of wind pollination. *Botanical Review* 51: 328–386.

NIKLAS, K. J., AND S. L. BUCHMANN. 1987. Aerodynamics of pollen capture in two sympatric *Ephedra* species. *Evolution; International Journal of Organic Evolution* 41: 104–123.

NIKLAS, K. J., S. L. BUCHMANN, AND V. KERCHNER. 1986. Aerodynamics of *Ephedra trifurca.* I. Pollen grain velocity fields around stems bearing ovules. *American Journal of Botany* 73: 966–999.

NIKLAS, K. J., AND V. KERCHNER. 1986. Aerodynamics of *Ephedra trifurc*a II. Computer modelling of pollination efficiencies. *Journal of Mathematical Biology* 73: 966–979.

NIKLAS, K. J., AND H.-C. SPATZ. 2012. Plant physics. University of Chicago Press, Chicago, Illinois, USA.

NORBÄCK-IVARSSON, L. 2014. Pollen morphology in *Ephedra* (Gnetales) and implications for understanding fossil ephedroid pollen from the Tibetan Plateau, using a phylogenetic approach. Master thesis, Stockholm University, Stockholm, Sweden.

OSBORN, J. M., T. N. TAYLOR, AND M. R. DE LIMA. 1993. The ultrastructure of fossil ephedroid pollen with gnetalean affinities from the Lower Cretaceous of Brazil. *Review of Palaeobotany and Palynology* 77: 171–184.

OSBORN, J. M., T. N. TAYLOR, AND E. L. SCHNEIDER. 1991. Pollen morphology and ultrastructure of the Cabombaceae: Correlations with pollination biology. *American Journal of Botany* 78: 1367–1378.

PAGEL, M. 1999. Inferring the historical patterns of biological evolution. *Nature* 401: 877–884.

PORSCH, O. 1910. *Ephedra campylopoda* C.A. Mey., eine entomophile Gymnosperme. *Berichte der Deutschen Botanischen Gesellschaft* 28: 404–412.

PUNT, W., P. HOEN, S. BLACKMORE, AND A. LE THOMAS. 2007. Glossary of pollen and spore terminology. *Review of Palaeobotany and Palynology* 143: 1–81.

R DEVELOPMENT CORE TEAM. 2014. R- A language and environment for statistical computing, version 3.1.1. R Foundation for Statistical Computing, Vienna, Austria. Website http://www.r-project.org/.

ROWLEY, J. R. 1995. Are the endexines of pteridophytes, gymnosperms and angiosperms structurally equivalent? *Review of Palaeobotany and Palynology* 85: 13–34.

RYDIN, C., A. KHODABANDEH, AND P. K. ENDRESS. 2010. The female reproductive unit of *Ephedra* (Gnetales): Comparative morphology and evolutionary perspectives. *Botanical Journal of the Linnean Society* 163: 387–430.

RYDIN, C., AND P. KORALL. 2009. Evolutionary relationships in *Ephedra* (Gnetales), with implications for seed plant phylogeny. *International Journal of Plant Sciences* 170: 1031–1043.

RYDIN, C., K. R. PEDERSEN, AND E. M. FRIIS. 2004. On the evolutionary history of *Ephedra*: Cretaceous fossils and extant molecules. *Proceedings of the National Academy of Sciences, USA* 101: 16571–16576.

SCHWENDEMANN, A. B., G. WANG, M. L. MERTZ, R. T. MCWILLIAMS, S. L. THATCHER, AND J. M. OSBORN. 2007. Aerodynamics of saccate pollen and its implications for wind pollination. *American Journal of Botany* 94: 1371–1381.

SCHLUTER, D., T. PRICE, A. Ø. MOOERS, AND D. LUDWIG. 1997. Likelihood of ancestor states in adaptive radiation. *Evolution* 51: 1699–1711.

STEEVES, M. W., AND E. S. BARGHOORN. 1959. The pollen of *Ephedra. Journal of the Arnold Arboretum* 40: 221–255.

TAKASO, T. 1990. "Pollination drop" time at the Arnold Arboretum. *Arnoldia* 50: 2–7.

TEKLEVA, M. V., AND V. A. KRASSILOV. 2009. Comparative pollen morphology and ultrastructure of modern and fossil gnetophytes. *Review of Palaeobotany and Palynology* 156: 130–138.

TREVISAN, L. 1980. Ultrastructural notes and considerations on *Ephedrites, Eucommiidites* and *Monosulcites* pollen grains from Lower Cretaceous sediments of southern Tuscany (Italy). *Pollen et Spores* 22: 85–132.

VAN CAMPO, M., AND B. LUGARDON. 1973. Structure grenue infratectale de l'ectexine des pollen quelques Gymnospermes et Angiospermes. *Pollen et Spores* 15: 171–187.

WETSCHNIG, W., AND B. DEPISH. 1999. Pollination biology of *Welwitschia mirabilis* Hook. f. (Welwitschiaceae, Gnetopsida). *Phyton* 39: 167–183.

WHITEHEAD, D. R. 1983. Wind pollination: Some ecological and evolutionary perpespectives. *In* L. Real [ed.], Pollination biology, 97–108. Academic Press, London, UK.

WODEHOUSE, R. P. 1935. Pollen grains; their structure, identification and significance in science and medicine. McGraw-Hill, New York, New York, USA.

VOGEL, S. 1981. Life in moving fluids: The physical biology of flow. Willard Grant Press, Boston, Massachusetts, USA.

ZAVADA, M. S. 1984. Angiosperm origins and evolution based on dispersed fossil pollen ultrastructure. *Annals of the Missouri Botanical Garden* 71: 444–463.

ZAVADA, M. S., AND N. GABARAYEVA. 1991. Comparative pollen wall development of *Welwitschia mirabilis* and selected primitive angiosperms. *Bulletin of the Torrey Botanical Club* 118: 292–302.

Appendix 1. Material used for scanning electron microscopy (SEM) and scanning transmission electron microscopy (STEM) investigations. Vouchers located at the British Museum of Natural History (BM), Harvard University Herbaria (HUH), National Herbaria of the Netherlands (L), New York Botanical Garden (NY), Swedish Museum of Natural History (S), Natural History Museum, Vienna (W), University of Vienna (WU).

No.	Taxon	Voucher	Collection information	SEM	STEM
700	*E. distachya*	J. Prudhomme 89 (WU)	Spain, 1989	*	*
764	*E. distachya*	K. Bolinder 764 (S)	Greece, 2012	*	*
603	*E. distachya*	Rechinger 53066 (W)	Persia, 1975	*	
108	*E. distachya*	Flora Germanica Exsicatae 7513 (HUH)	Germany, 1903	*	
542	*E. foeminea*	K. Bolinder 542 (S)	Greece, 2012	*	*
307	*E. foeminea*	L. Norbäck-Ivarsson & O. Thureborn (S)	Croatia, 2013	*	*
190	*E. foeminea*	R. Pampaninio & R. Pichi-Sermolli 139 (L)	Libya, 1934	*	
712	*E. foeminea*	F.S. Meyers & J.E. Dinsmore 8124 (L)	Palestine, 1912	*	
573	*E. foeminea*	O. Porsch (WU)	Croatia, 1910	*	
64	*E. likiangensis*	K. Bolinder 64 (S)	In cultivation, Stockholm University, 2011		*
465	*E. likiangensis*	J.F. Rock 3694 (NY)	China, 1922	*	
706	*E. likiangensis*	G. Forrest 5564 (BM)	China, 1910	*	
291	*E. nevadensis*	I.W. Clokey 6509 (S)	USA, 1935	*	*
288	*E. nevadensis*	C. Epling & W. Robinson (S)	USA, 1932	*	
450	*E. nevadensis*	L.S. Rose 58108 (S)	USA, 1958	*	
454	*E. trifurca*	R.D. Worthington 24587 (NY)	USA, 1995	*	*
446	*E. trifurca*	A. Nelson 1619 (NY)	USA, 1935	*	
445	*E. trifurca*	M.C. Johnston et al., 10573 (NY)	Mexico	*	
236	*E. trifurca*	P. Allen (S)	USA, 1934	*	
134	*E. trifurca*	C.V. Hartman 642 (HUH)	Mexico, 1891	*	
63	*E. viridis*	K. Bolinder 63 (S)	In cultivation, Stockholm University, 2011		*
246	*E. viridis*	L.S. Rose 58080 (S)	USA, 1958	*	
427	*E. viridis*	J.L. Reveal 100 (NY)	USA, 1962	*	
439	*E. viridis*	Neely 4353 (NY)	USA, 1980	*	
136	*E. viridis*	J.T. Howell 3824 (HUH)	USA, 1928	*	
216	*Welwitschia mirabilis*	K. Bolinder 216	In cultivation, Bergius Botanic Garden, 2013		*